Design Engineering

ISSN: 0011-9342 | Year 2021
Issue: 8 | Pages: 1032-1044

Numerical Investigation for Turbulent Flow through a Solar Air Heater Channel with a Different Curved Baffles Geometry and Position

Nabeel N. Al-Mayyahi[1*], Firas lattefhussany[1] and Radhwan Ali[1]
[1]Department of Mechanical Engineering, University of Misan, Iraq
Corresponding author e-mail (nabeelclick@uomisan.edu.iq)

Abstract. The present paper numerically investigates the turbulent flow and heat transfer improvement in the solar air heater duct. Ansys Fluent software is used to solve the 3-dimensional turbulence models of three different curved baffles geometry attached inside the duct and examined to enhance the heat transfer between the heated absorber surface and the air passing in two directions for Reynolds number (Re) ranged between 8000 to 20000. The average Nussle number (Nu), the friction factor (f), and the performance Factor (P.F) are calculated to clarify the performance of the models.Results show that the geometry design and position of the curved baffle have a significant effect in generating and strengthening the vortices inside the duct leading to enhance heat transfer. Besides that, the contrariwise position baffle that extending in height at the ends and shrinking in the middle of geometry (OC3) gives a clear enhancement as compared with other models. The maximum P.F of the OC3 baffle model ranged between (2.16 to 1.6).
Keywords: Solar air heater, Curved baffles, Friction factor, Performance factor.

1. Introduction

There is much application that used solar energy for useful used such as in water heater, heating and refrigeration systems, power and solar air heaters (SAH) systems. The latter is widely used in industrial and domestic applications, giving useful heat from solar energy because of its modest design, very little cost, and keeping it free [1].The boundary layer near the heated wall must be destroyed or decreased to obtain a high heat transfer between the circulation air and the heated duct surfaces. This can be achieved by increasing the turbulence of the fluid. Many types of tabulator devices used inside the duct to increase the fluid turbulence intensities by creating vortexes for the passing fluid such as fins, rib, and baffles. However, the devices increase the pressure drop due to the flow blockage effect.

Many researchers have been studied for these issues to enhance the heat transfer in an absorber plate. For instance, Sriromreun et al. [2] The experimental and numerical techniques were combined to research the heat transfer enhancement of the pipe flow field with Z-shaped baffles. The study found that the improvement in the heat transfer of the in-phase Z-shaped baffles was larger than the Z-shaped out-phase baffles. The simulation of Jin et al. [3] helical vortex flows could be produced by indicated multi V-shaped ribs, promoting the fluid mix among the colder above channels fluid and the heater near-bottom-wall fluid.Wen et al. [4] For jagged fin geometry optimization analyses, the response surface method, and genetic algorithm were used. The results concluded that the heat exchanger produced by the optimization process increased the rate of heat transfer by 145% and decreased energy consumption by 48.5%. Kumar et al. [5] The airflow was analysed in the V-shaped ribs through a heater plate with several gaps. This method has been found to allow the secondary flow to converge more quickly with the mainstream to improve the efficiency of heat transfer. Sharad and Saini [6] The arc-shaped ribs attached to the absorber plate were numerically investigated and the absorber plate was subjected to a constant heat flux of 1000 W/m2. Parameters ranged from 6000 to 18,000 with (Re). Ravi et al. Jheng-Long et al [7] Conduct a numerical simulation for optimizing the performance case in the solar station with multi of them V-shaped baffles in a turbulent flow. It was attained by the enhanced design

ISSN: 0011-9342 | Year 2021
Issue: 8 | Pages: 1032-1044

of baffles has a 12% of enhancement for performance factor 12% as compared with a standard multi V-shaped baffle.

Through this study, the heat transfer increased by inserting different tabulator's designs and also the pressure drop of the channel flow is increased due to the decrease flow area effects. Therefore, the present paper discusses the thermal-hydraulic performance in a(SAH) duct by inserting different geometries of the curved baffle for heat transfer enhancement and possibly for reducing the pumping power required. The numerical simulation was adopted by CFD code for solving the governing equations of the 3D models.

2. Description of problem statement and treatment

2.1.The system description

The curved baffles are inserted inside the solar air heater channel and tested. The baffles are fixed at the bottom side of the absorber plate as shown in the schematic in figure1. The channel length is divided into three sections: entry Li=500 mm, absorber length L = 400 mm, and exist Le = 1000 mm. The channel high and width is H=30 mm and W=120 mm respectively. Different three curved baffles geometries that were taken up for investigation are listed in figure2. The baffle is constant in height (e) is 10mm for the C1 baffle model. The baffle was extended in height (e*2) at the middle beside that, the side of the ends is halved at the other side (e/2) as in model C2. But in the C3 model, the baffle height was extended at the end and halved at the middle. Moreover, all the mentioned baffles were discussed above are modeled but in contrariwise position (opposite direction) on the absorber plate as in OC1, OC2, and OC3 models. All the baffles have nearly surface area with a maximum difference is 2.8% as compared in each model. The air passing through the channel in one direction at an inlet temperature, Tin= 27°C and leave it at Tout. A uniform heat flux subject on an absorber is constantly equal to 1000 w/m². The baffles geometries are tested at different Reynolds numbers was ranging from 8000 to 20000. The investigation was done using software ANSYS 19.0.

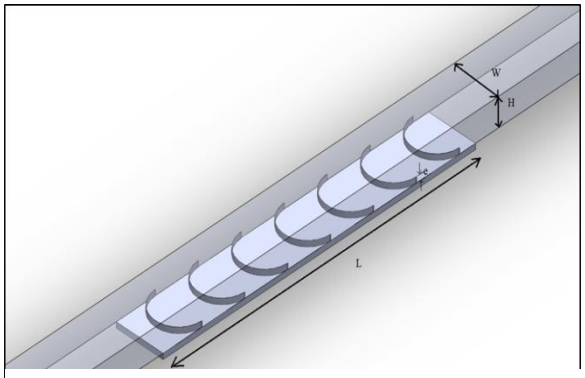

Figure1. The (SAH) model with an inclined curved baffle.

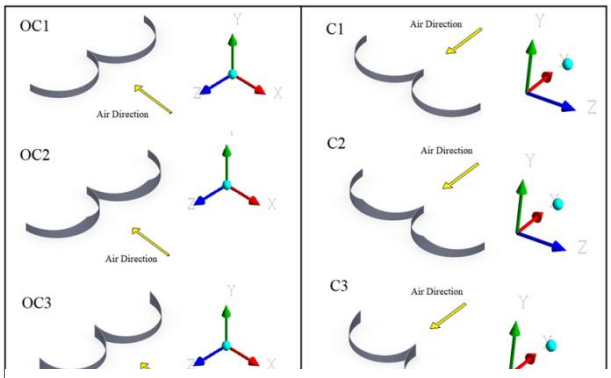

Figure 2. View of curved baffles with different geometries and directions.

2.2. The Governing and the Theoretical Equations

The numerical model for fluid flow and heat transfer in the SAH channel was developed under the following assumptions:

•A three-dimension, incompressible, and steady-state for fluid flow and heat transfer.
•Adiabatic baffles.
•The fluid is turbulence.
•The radiation effect was neglected.

ISSN: 0011-9342 | Year 2021
Issue: 8 | Pages: 1032-1044

•No-slip condition and uniform inlet air velocity.

According to the above assumptions, the following Naiver Stokes and energy equations are giving below, which are written in the following.

The continuity equation:

$$\frac{\partial \rho ui}{\partial x_i} = 0 (1)$$

The equation of the momentum is:

$$\frac{\partial (\rho u_i u_j)}{\partial x_j} = \frac{\partial p}{\partial x_i} + \frac{\partial}{\partial x_j}\left[\mu\left(\frac{\partial u_i}{\partial x_j} + \frac{\partial u_j}{\partial x_i}\right) - \rho u_i u_j\right] \quad (2)$$

And the equation of the energy for fluid is:

$$\rho C_p u_j \frac{\partial T}{\partial x_j} = \frac{\partial}{\partial x_j}\left(k_f \frac{\partial T}{\partial x_j} + \rho u_j C_p u_j T\right) \quad (3)$$

For the solid:

$$\frac{\partial}{\partial x_i}\left(k_s \frac{\partial T}{\partial x_i}\right) (4)$$

In CFD simulations, several turbulence models are available to simulate turbulent flow behavior. Added equations are specified and solved to compute turbulence-related quantities by selecting the appropriate model under specific conditions. A typical k-ε model turbulence modeling is selected in the present study that transports the turbulent kinetic energy equation and its dissipation rate, which are written as follows, respectively [7].

$$\rho u_j \frac{\partial k}{\partial x_j} = \frac{\partial}{\partial x_j}\left[\frac{\mu_t \partial k}{\sigma k \partial x_j}\right] + G_k - \rho\varepsilon (5)$$

$$\rho u_j \frac{\partial \varepsilon}{\partial x_j} = \frac{\partial}{\partial x_j}\left[\frac{\mu_t \partial \varepsilon}{\sigma \varepsilon \partial x_j}\right] + C_{1\varepsilon}\frac{\varepsilon}{k} G_{k+} C_{2\varepsilon}\rho\frac{\varepsilon^2}{k} (6)$$

Where

$$G_{k=}\mu_t\left[\frac{\partial ui}{\partial x_j} + \frac{\partial uj}{\partial xi}\right]\frac{\partial ui}{\partial x_j} \quad (7)$$

And

$$\mu_t = C_\mu \rho \frac{k^2}{\varepsilon} (8)$$

The factors constant values are in the following values:

$$\sigma k = 1.0,\ \sigma\varepsilon = 1.3, C_\mu = 0.09 C_{1\varepsilon} = 1.44,\ C_{2\varepsilon} = 1.92 \quad (9)$$

3.Numerical method

The Ansys Fluent (19.0) software was used to build the geometry and generate the mesh of the mathematical model as shown in figure3. A Cartesian cut cell mesh method type was adopted that generated by cutting the solid bodies out of a background Cartesian mesh [8]. The mesh treatment is done by taking into consideration the baffles curvatures and the regions between the puzzles and absorber of the channel in command to detention the details of boundary layer flow. The number of grids was increased by a factor of about 2 to verify the grid independence. The computational domain's initial three-dimensional mesh had 1,423,456 cells. Then, the number of cells was increased from 2,895,146 cells to 5,811,126 cells**.** Finally, at themesh dependency test**,** the 2,895,146 cells give stable results with less computational time. To solve the governing equations, the programming code used is based on the finite volume method (FVM). The Basic (Semi Implicit Method for Pressure Related Equation) algorithm was used for the pressure-velocity coupling. The diffusion term was approximated by the second-order central difference scheme in the momentum and energy equations, giving a stable solution. A second-order upwind method for the discretization of convection terms

ISSN: 0011-9342 | Year 2021
Issue: 8 | Pages: 1032-1044

was also introduced. The residual target for the equations of continuity, momentum, and energy was (10-7). Until the fixed residuals were obtained or when they stabilized at constant values, the governing equations were iteratively solved. Around 1300-1500 iterations are required for most simulations.

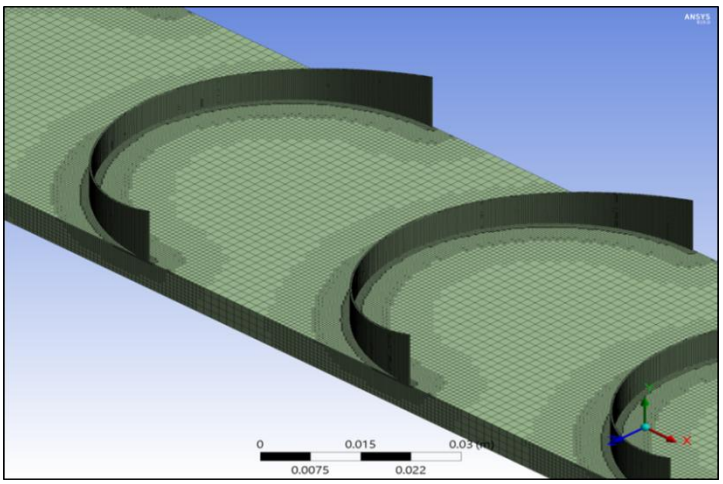

Figure 3.Mesh grid of generation symmetric at C3 matrix model.

4. Performance parameters

The theoretical equations in the present that declining the thermal-hydraulic performance for various models of SAH, which are dimensionless parameters are given in the following equations. The Reynold number (Re) based on the channel hydraulic diameter is defined as the equation (10):

$$\boldsymbol{Re}=\frac{\boldsymbol{\rho}.\boldsymbol{D_h}.\boldsymbol{v}}{\boldsymbol{\mu}} \quad (10)$$

And

$$D_h = \frac{2.w.h}{w+h} \quad (11)$$

The average heat transfers coefficient h for the absorber plate is:

$$h = \frac{q\ Aa.}{A.(Tw-Ta)} \quad (12)$$

Where

$$Ta = \frac{(T_{ip}+T_{op})}{2} \quad (13)$$

To find the average Nusselt number (Nu), the equation (14) is used based on used the fluid thermal conductivity and other previous equations (11) and (12)

$$Nu = \frac{\mathrm{h}.D_h}{Kf} \quad (14)$$

The friction factor for the channel is calculated from the pressure drop and the inlet velocity as the equation:

$$f = \frac{\Delta P.D_h}{2\ .L.\rho.v^2} \quad (15)$$

The thermal performance factor (P.F) is defined as the ratio of the heat transfer coefficient and pumping power based on the smooth and other models.

$$P.F = \left[\frac{N}{Nu_s}\right] * \left[\frac{f}{f_s}\right]^{-0.33} \quad (16)$$

ISSN: 0011-9342 | Year 2021
Issue: 8 | Pages: 1032-1044

5. Results and discussion

Different three curved baffles models C1, C2, and C3 on thermal-hydraulic performances have been investigated at four different Re numbers which ranging between (8000 to 20000). Moreover, the same baffles geometry and numbering are tested but in opposite direction in models OC1, OC2 and OC3 and discussed below. These models are compared numerical with smooth model and validate against the experimental results.

5.1. Validation of the CFD model

The smooth model validation is performed by comparing the local Nusselt number and friction factor predicted by the experimental work of smooth air channel of the literature [9]. Moreover, the same turbulence model is verified with the same turbulence model air duct at reference [7] as shown in figure 4. The results show in good agreement with literature results with maximum error against experimental and numerical results are 22% and 12% of Nu in respectively, moreover, an expected trend for friction factor. Thus, the current numerical model has been employed to simulate the hydrothermal flow in the solar air channel.

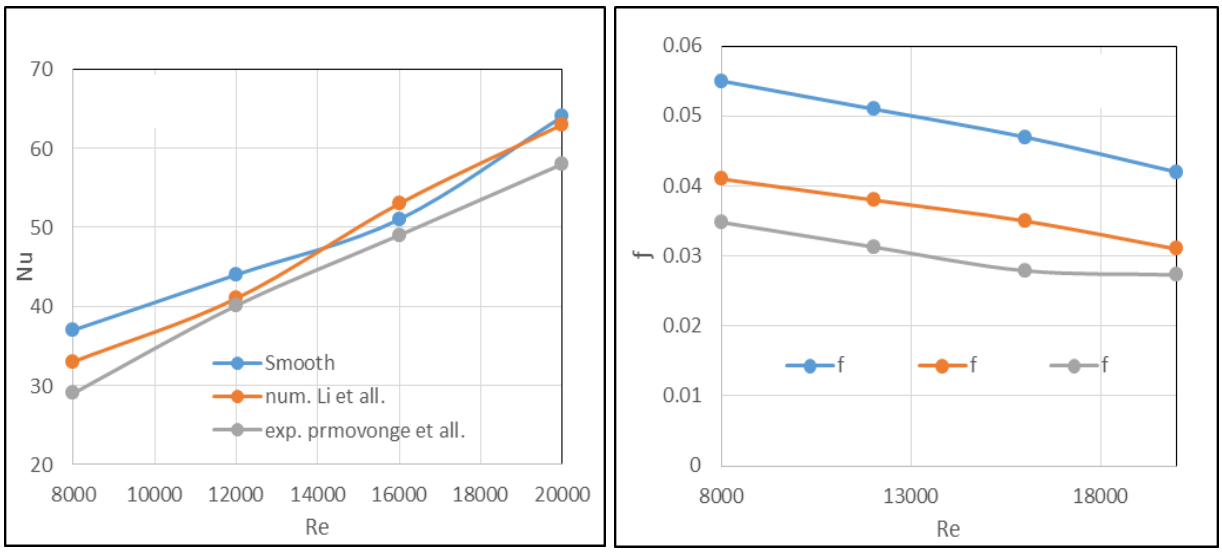

Figure 4. Numerical validation of present numerical results against experimental and numerical predicted results (a) Nu and (b) f.

5.2. Flow field and Thermal profile

For flow field investigation in different models, figure 5 presents the turbulent kinetic energy for the three model cases C1, C2, and C3 with a constant value of Reynolds number equal to 12,000. Generally, the highest turbulent energy occurs at the beginning of the absorber and then decreased with distance. The C2 model gives the highest turbulent energy which is expected due to extend baffle height in the middle that obstructs the airflow in the baffle bounded area. On the other hand, figure6 shows the baffles on the opposite side that ceases OC1, OC2, and OC3. The turbulent energy is high at OC3 for the same reason as discussed which the baffle extended in height at the ends. Another flow field investigation is in figure 7 and figure 8, which present the air velocity contours at different baffle planes. As seen the velocity increased at the baffle center in cases C1, C2, and C2 while the velocity increased at the baffles ends at OC1, OC2, and OC3. This clearly shows that the baffle position is affected by the airflow direction. Its clear nothing the velocity magnitude at the centreline in themodels OC1, OC2, and OC3 is high than other models, thus giving a better chance for decrease the thermal boundary layer and thus the heat transfer improved.

Design Engineering

ISSN: 0011-9342 | Year 2021
Issue: 8 | Pages: 1032-1044

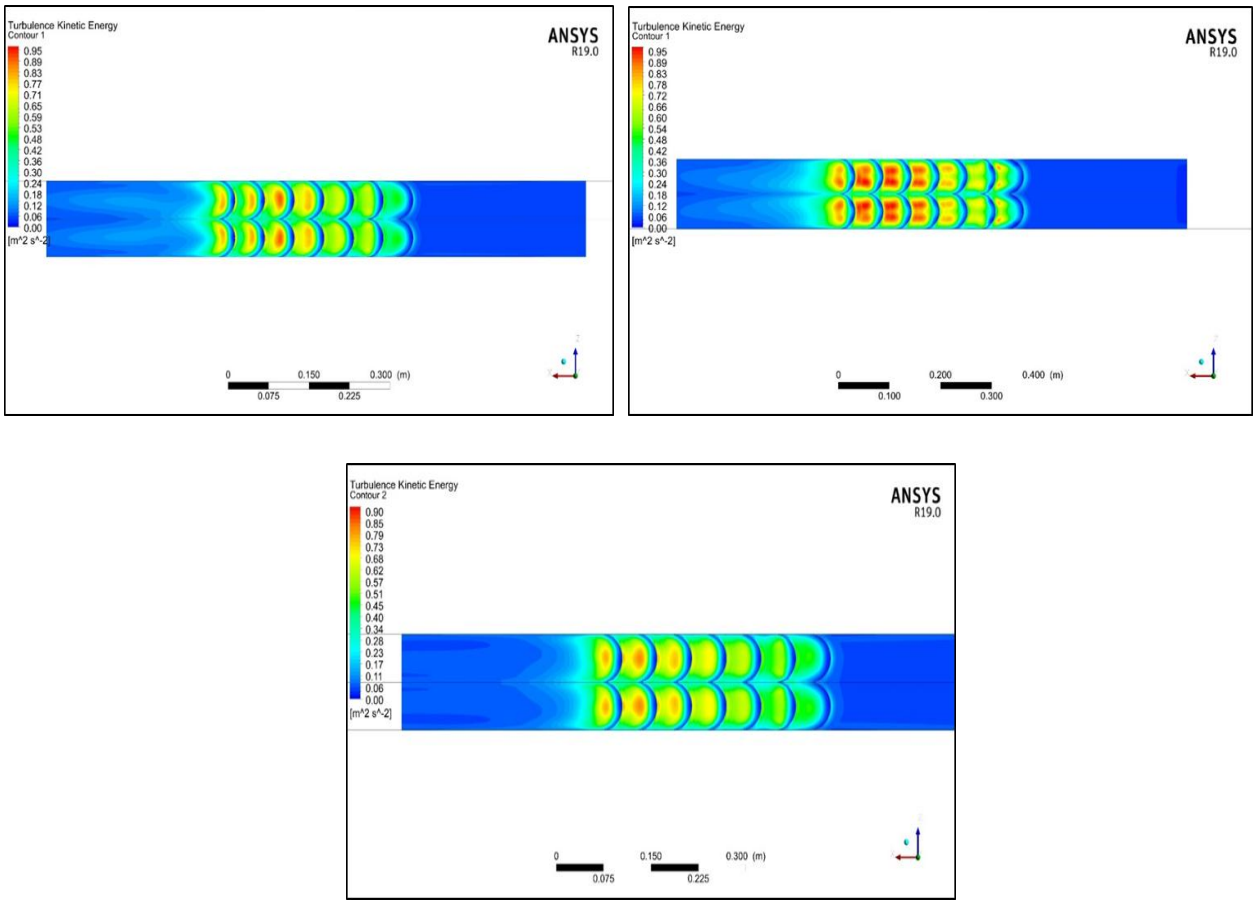

Figure 6. Turbulence kinetic energy contours for various baffle geometry in models (a) OC1, (b) OC2, and (c) OC3.

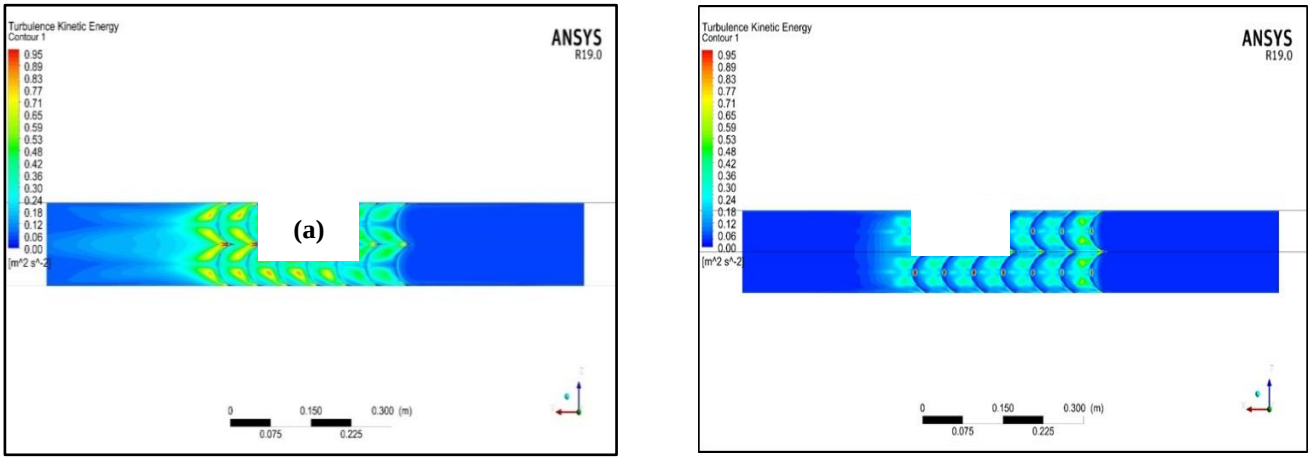

Design Engineering

ISSN: 0011-9342 | Year 2021
Issue: 8 | Pages: 1032-1044

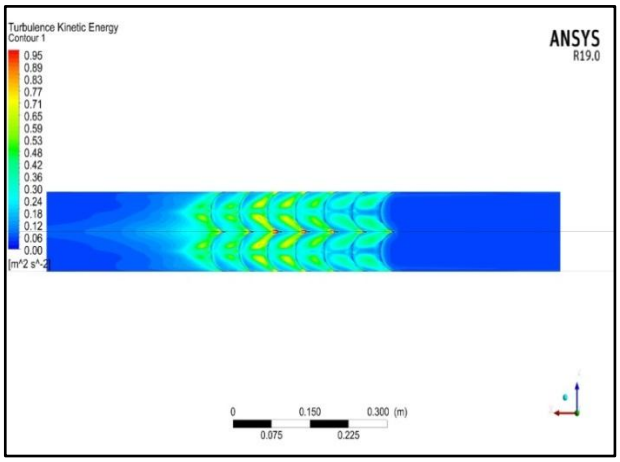

Figure 7. Air velocity contours for various baffle geometry in models (a) C1, (b) C2, and (c) C3

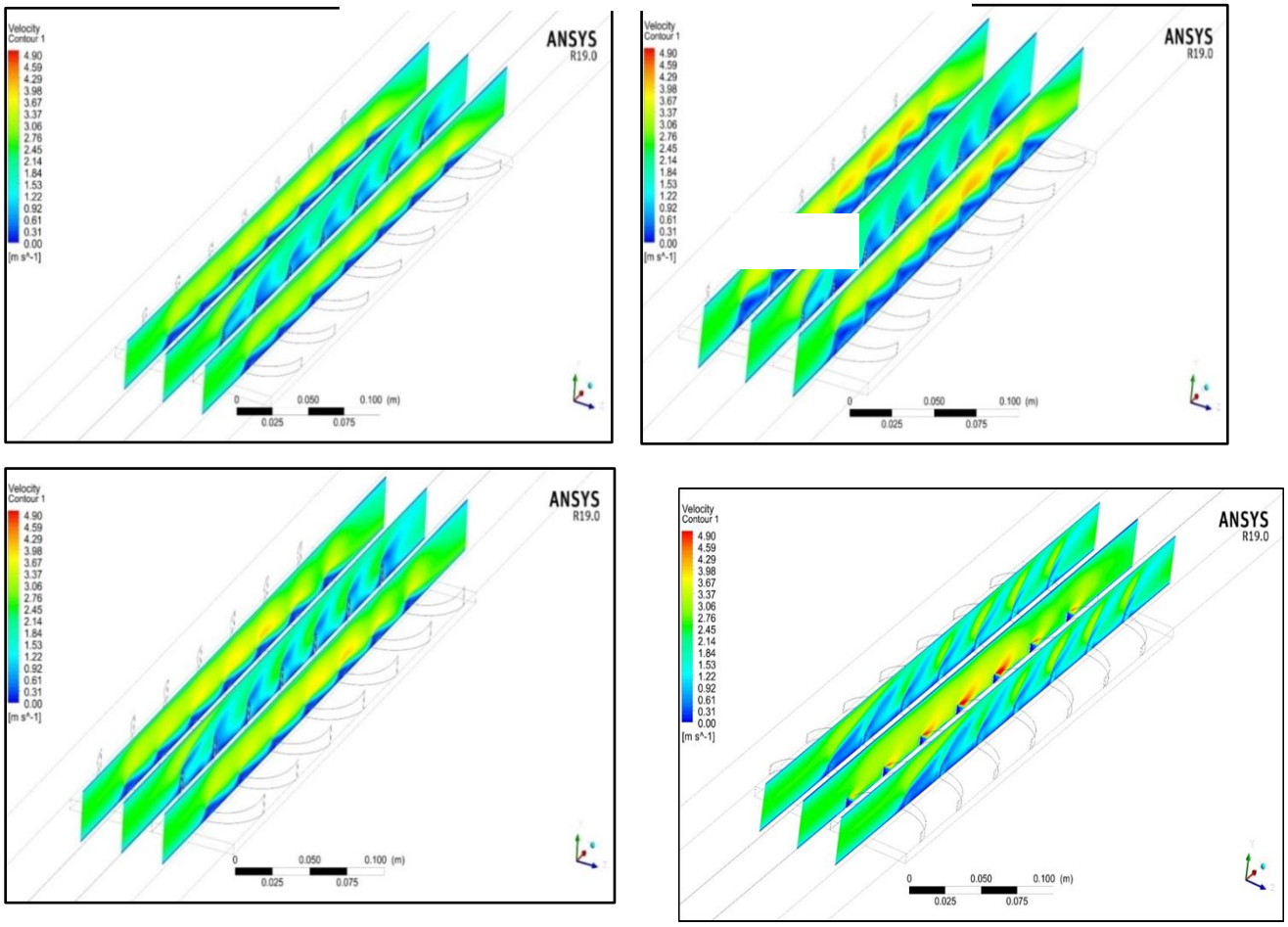

Design Engineering

ISSN: 0011-9342 | Year 2021
Issue: 8 | Pages: 1032-1044

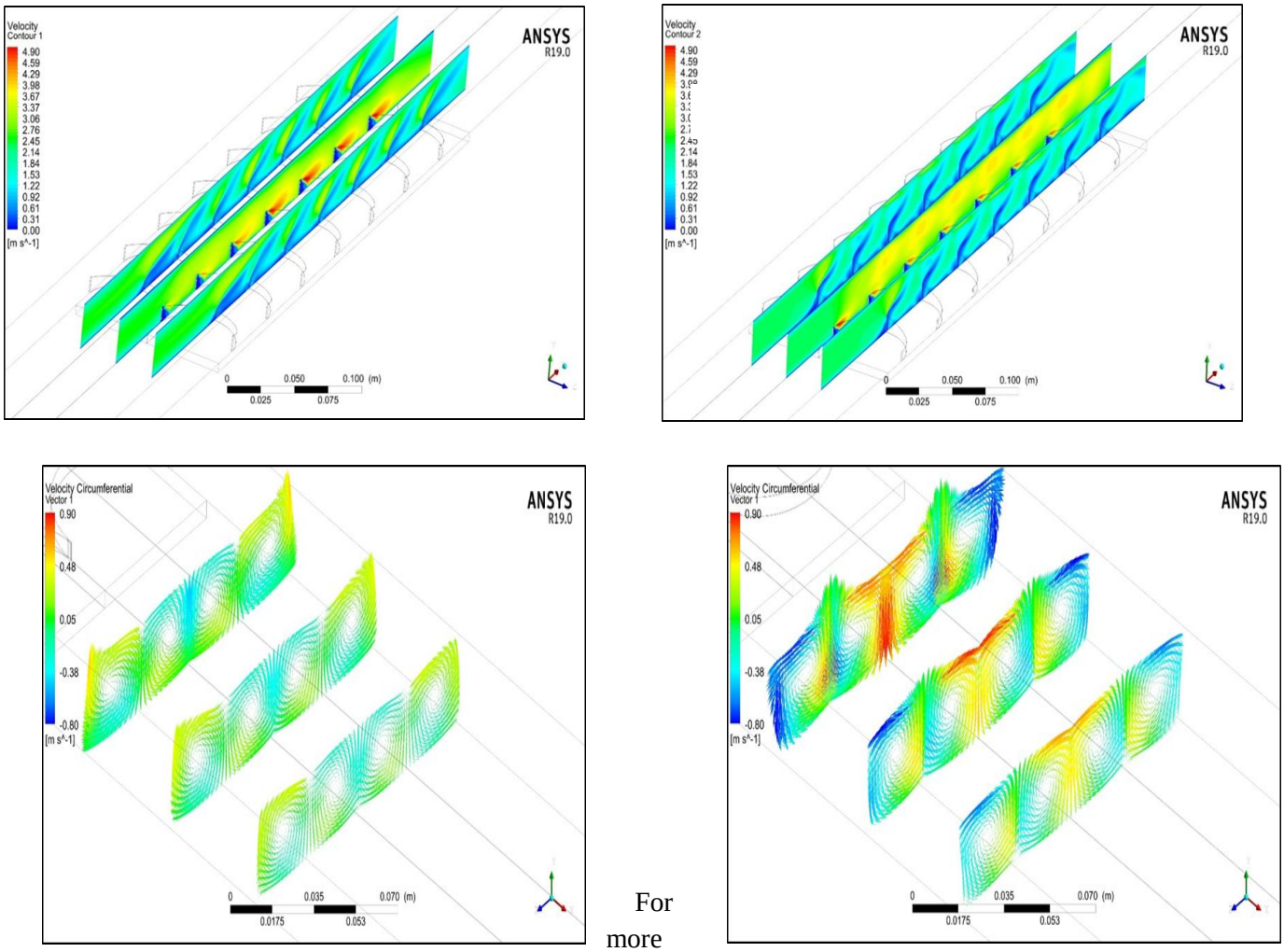

Figure 8. Air velocity contours for various baffle geometry in models (a) OC1 (b) OC2 and (c) OC3

details on the flow structure inside the channel, figure 9 described the velocity vector for two models C1 and OC1. Different planes inside the channel are viewed, each plane located in the middle between two baffles. Generally, four vortices are seen in each plane that indicates curved baffles affect increasing the turbulence of the fluid flow. It's worth mentioning that the flow structure is different in each model, that the velocity direction at the centreline of the absorber in C1 is down (toward the plate), and at the sides, vertical velocity raised (toward the upper channel), meanwhile the velocity direction at OC1 is inversely situated compared to C1 model. Moreover, the velocity magnitude is different in each model that the intensity of the vortex in OC1 is larger than in the C1 model.

For the thermal investigation,figure10 andfigure11 show the temperature contour for the three models and the models with the opposite side in respectively at fixed Re number value of 12000. It is seen that the plate surface temperatures following the first baffle region are lower than that at the absorber entrance region. This attributed to the vortex formation that occurred in the area following the first baffle as a consequence of air impingement on the first baffle leading to remove the accumulated heat in that area The last region on the

Design Engineering

ISSN: 0011-9342 | Year 2021
Issue: 8 | Pages: 1032-1044

absorber that the thermal boundary increased lengthways the length of the channel. The absorber natural surfaces are extracted in each model and the lowest for the three models : 51.7 °C, meanwhile, at the baffles opposite direction; the OC3 is the lowest, which is 47.9 °C.

Figure 9. Compaction for velocity distribution at various two models (a) C1 and (b) OC1

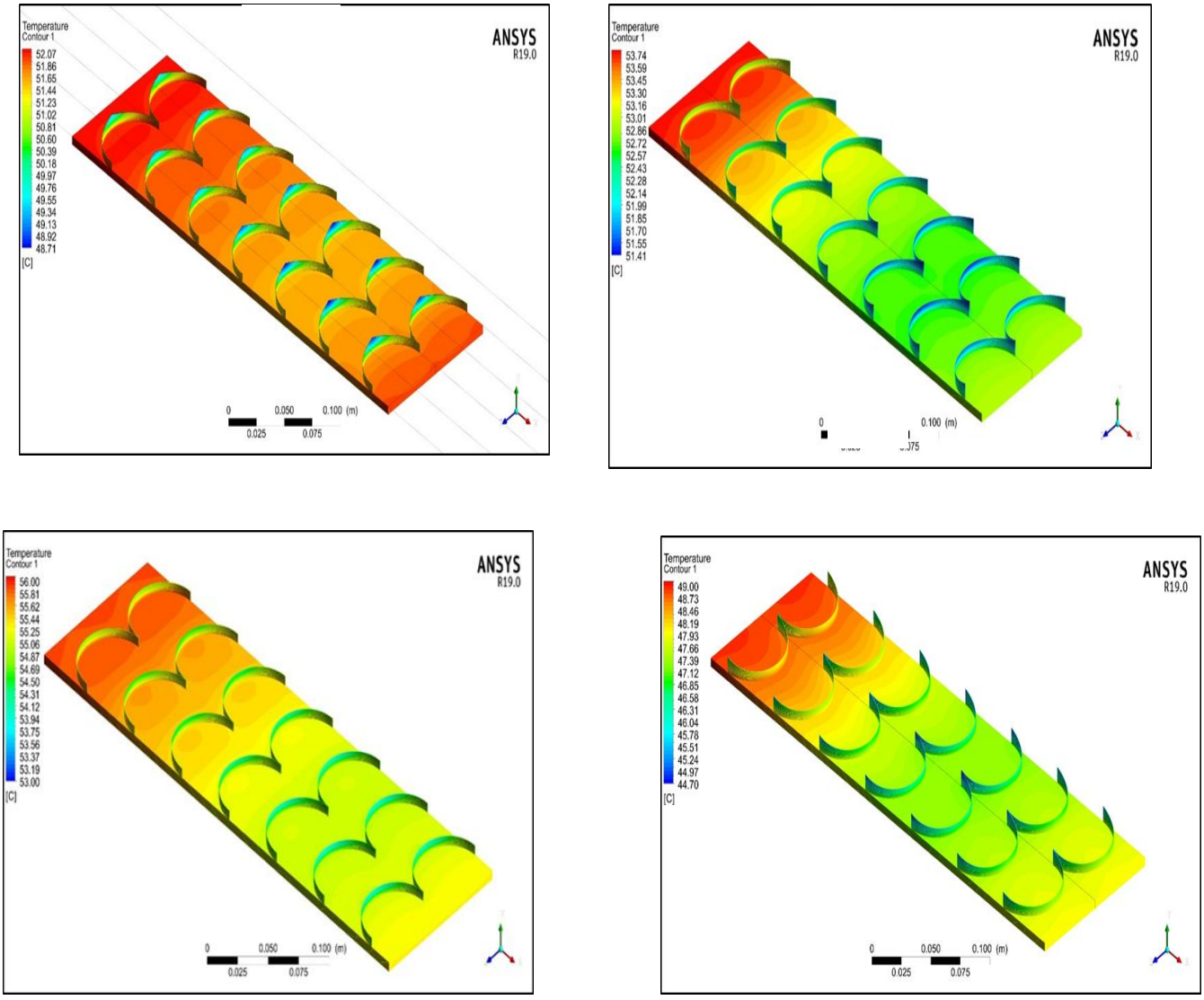

Design Engineering

ISSN: 0011-9342 | Year 2021
Issue: 8 | Pages: 1032-1044

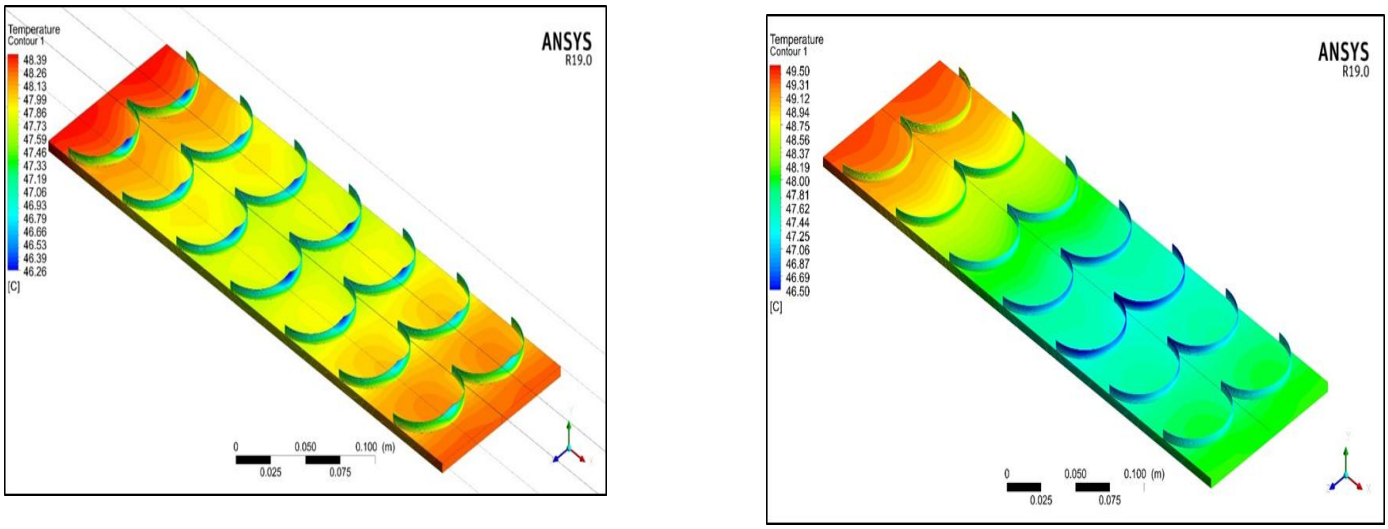

Figure 11. Temperature contours for various baffle models (a) OC1 (b) OC2 and (c) OC3

5.3. Thermo hydraulic performance

Figure 12 presents the variation of the friction factor f with the mentioned range of Reynolds numbers for various baffles models. As expected the trend of friction factor decrease with Re number resulting in a high-pressure drop occurs. The opposite position baffles models have an extreme increment of f in comparison with the original baffle. Figure 13 plots the values of the average Nu number with Re number for different baffle cases. As expected, the increment of Nu increases with the Re number due to the air kinetic energy turbulence increased. The Nu number trends to rise for OC1, OC2, and OC3 are more than the original models. The model that will result in maximum improvement in heat transfer with a minimum pressure drop penalty must be determined. Therefore, the P.F curves are plates as in figure 14a for C1, C2, and C3 models, and the three same baffles but in opposite direction as in figure 14b.

ISSN: 0011-9342 | Year 2021
Issue: 8 | Pages: 1032-1044

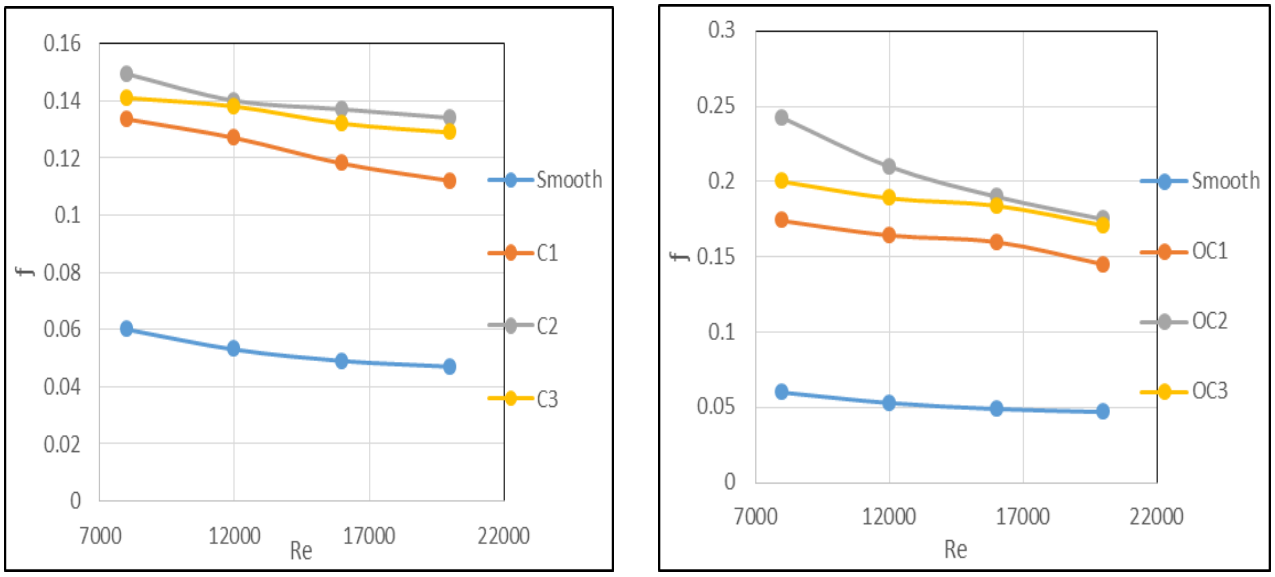

Figure 12. The variation of *f* with Reynolds number in different baffle models of SAH (a) Three baffles models numbering and (b) same baffles numbering but in the opposite side position.

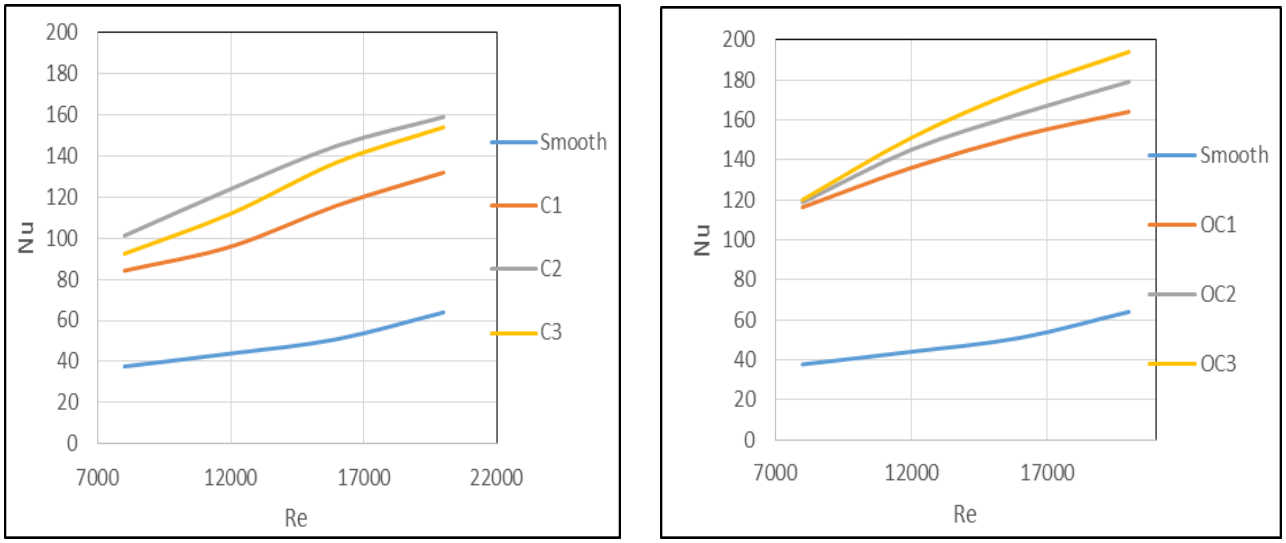

Figure13. The variation of Nu with Reynolds number in different baffle models of SAH (a) Three baffles models numbering and (b) same baffles numbering but in the opposite side position.

ISSN: 0011-9342 | Year 2021
Issue: 8 | Pages: 1032-1044

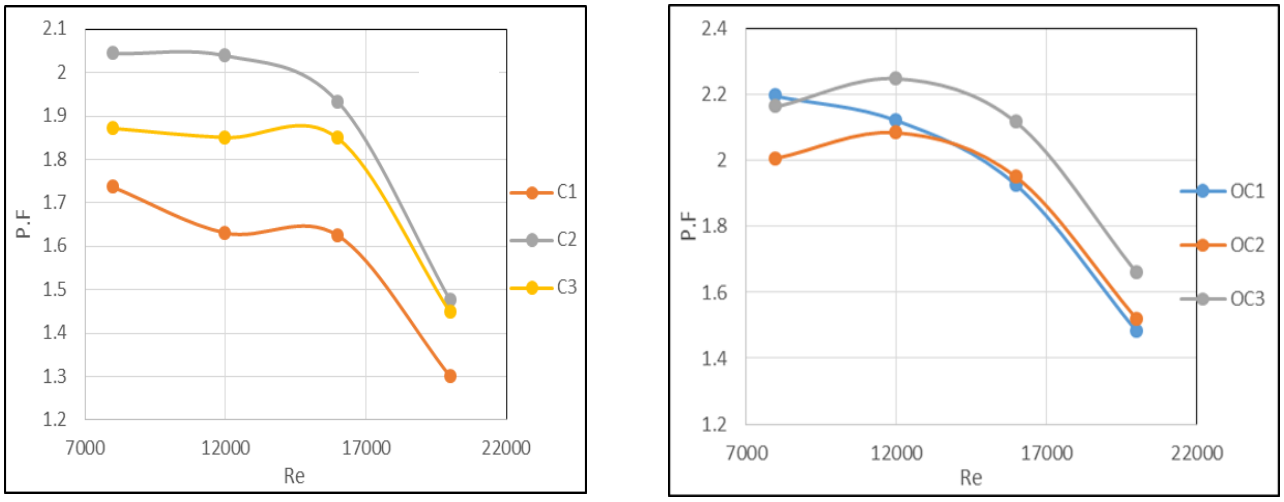

Figure14. The variation of P.F with Reynolds number in different baffle models of SAH (a) Three baffles models numbering and (b) same baffles numbering but in the opposite side position.

6. Conclusions

The present study summarized the results of a numerical computational study of turbulent flow and heat transfer characteristics in a SAH channel fitted with different curved geometry in two directions.

The working fluid is air flowing through the channel at Reynolds number which varies from 8000 to 20000. The baffles at opposite side positiongive a better heat transfer than the original model and however with additional pressure drop. Moreover, the OC3 model is provides a significant increase in heat transferperformance Factor (P.F = 2.16 to 1.6) over the smooth model, which the Nu found to be around 64% higher.Hence, the higher Nu number occurs at placed baffle in the opposite direction since the intensity of vortex is more powerful leading to a decrease in the thermal boundary layer.

References

[1] T. Alam, M.-H. Kim,Numerical study on thermal-hydraulic performance improvement in solar air heater duct with semi ellipse-shaped obstacles. Energy 112 (2016) 588-598

[2] ParkpoomSriromreun, ChinarukThianpong, PongjetPromvonge, Experimental and numerical study on heat transfer enhancement in a channel with Z-shaped baffles, Int. Commun. Heat Mass Transfer 39 (2012) 945–952.

[3] DongxuJin, Manman Zhang, Ping Wang, Xu Shasha, Numerical investigation of heat transfer and fluid flow in a solar air heater duct with multi V-shaped ribs on the absorber plate, Energy 89 (2015) 178–190.

[4] J. Wen, H. Yang, X. Tong, K. Li, S. Wang, Y. Li, Optimization investigation on configuration parameters of the serrated fin in a plate-fin heat exchanger using genetic algorithm, Int. J. Therm. Sci. 101 (2016) 116–125.

[5] Anil Kumar, R.P. Saini, J.S. Saini, Experimental investigation on heat transfer and fluid flow characteristics of airflow in a rectangular duct with multi V-shaped rib with gap roughness on the heated plate, Sol. Energy 86 (2012) 1733–1749

ISSN: 0011-9342 | Year 2021
Issue: 8 | Pages: 1032-1044

[6] Kumar S, Saini RP. CFD-based performance analysis of a solar air heater duct provided with artificial roughness. Renew Energy (2009); 5:1285-91.
[7] Long J,Wen Tang H,Yang Y. Numerical simulation and thermal performance optimization of turbulent flow in a channel with multi V-shaped baffles. International Communications in Heat and Mass Transfer 92 (2018) 39–50
[8] Ingram D., Causon D., MinghamC .Developments in Cartesian cut cell methods. Mathematics and Computers in Simulation 61 (2003) 561–572
[9] PongjetPromvonge. Heat transfer and pressure drop in a channel with multiple 60° V-baffles. International Communications in Heat and Mass Transfer 37 (2010) 835–840